



# Various Experimental Applications of Digital Image Correlation Method

S. Mguil-Touchal, F. Morestin, M. Brunet

*Laboratoire de Mécanique des Solides, INSA de Lyon, Bât. 304,  
69621 Villeurbanne, France*

*Email: lms@insa.insa-lyon.fr*

## Abstract

Despite the powerful of current calculus codes by finite element or analytical, their reliability and validity must be justified by experimental tests. An original software for the displacement field measurement is presented in this paper. This software use the digital picture correlation principle. Due to this technique, the accuracy of the measure could reach 1/60 th of a pixel and, it is possible to measure strains between  $5.10^{-5}$  to 0.8. Initially, this software was developed for measuring strains on a sheet testing in metal forming. But, it is revealed that this application field is more important : biomechanical field, geotechnical field, metal characterization, control tests, ..... This software could be used, nowadays, for all application which need the knowledge of displacement and strain field for a plane surface. Of course, the experimental conditions must be made in such a way that any deterioration of the random aspect, deposited on the piece, will occur. Lost, alteration or little modification of the speckle aspect will not guarantee the success of the measure. Finally, the purpose of this paper will be, first, to give clearly the mathematical principle of the displacement field determination by a correlation method. Then, various experimental tests using the correlation method, are presented. The powerful of this technique is show by their variety. This method of measure without contact can be an another tool for validating, in a short time, a numerical or analytical result.

## 1. Introduction

The accurate knowledge, without contact, of displacement field and/or strain field for a plane body is more and more researched. The new technique introduced in this paper for the displacement and strain field measurement have in the same time a very large strain range measurement and also a good accuracy on the displacement measurement. Also, this technique reduces the computation time due to a displacement field determination entirely computerized. A continuous information field could be obtained with an important density of the measured point : more than 15000 points for a field of

1024 by 1024 pixels. This new technique requires only a speckle aspect which could be put on the specimen in few seconds with a paint spray.

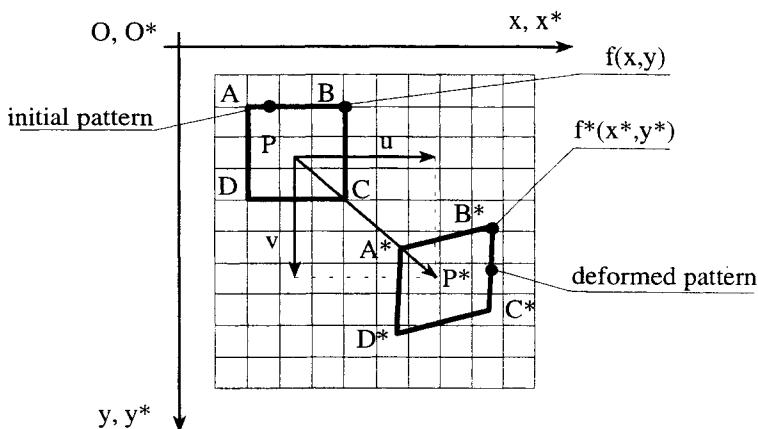
## 2. Method

### 2.1. Bibliography

This technique was principally developed by M. A. Sutton et al [1]. The following principles are used for a technique by digital picture correlation. The picture of the body could be represented by a discrete function : value between 0 and 255 of its grey levels. The correlation calculation are done for a subimage called pattern. The displacement field is supposed homogeneous inside the pattern. The initial picture representing the body before distortion is a discrete function noted  $f(x,y)$  will be transformed in an other discrete function noted  $f^*(x^*,y^*)$  after distortion or displacement. The theoretical relation between the two discrete functions could be written as :

$$f^*(x^*,y^*) - f(x + u(x,y), y + v(x,y)) = 0 \quad (1)$$

$u(x,y)$  and  $v(x,y)$  represent the displacement field for a pattern. The figure 1 presents different used definitions :



*For a better understanding, the initial and the deformed picture are represented in the same axis.*

Figure 1 : Notations

The four essential elements for a technical correlation are :

- the mathematical definition for the displacement field on a pattern which has to include, at the same time, the strain terms and the term of rigid body displacement,

- a mathematical correlation criterion between the two discrete functions  $f(x,y)$  and  $f^*(x^*,y^*)$ ,
- an interpolation method for the grey level of the pictures is needed in order to reach a sub pixel accuracy [2],
- the mathematical solution for the determination of the strain term for a pattern, [3-4].

## 2.2. Mathematical principle of the method

### 2.2.1. Choice for the displacement field [5]

The method uses the following displacement field because the research of all its terms (rigid body, strains) will be done by a bilinear interpolation. So, the displacement field for a pattern is taken homogenous and bilinear in  $x$  and  $y$  as

$$\begin{cases} u(x,y) = au \cdot x + bu \cdot y + cu \cdot x \cdot y + du \\ v(x,y) = av \cdot x + bv \cdot y + cv \cdot x \cdot y + dv \end{cases} \quad (2)$$

It contains the rigid body translation terms ( $du$  and  $dv$ ), the elongation terms ( $au$ ,  $av$  and  $bu$ ,  $bv$ ) and the shearing terms ( $cu$  and  $cv$ ).

### 2.2.2. Choice for the correlation coefficient

The most used correlation coefficient for a correlation technique are the least square and the crossed coefficients [6] :

$$C_1 = \int_{\Delta M} (f(x,y) - f^*(x^*,y^*))^2 \cdot dx \cdot dy \quad (3)$$

and

$$C_2 = 1 - \frac{\int_{\Delta M} f(x,y) \cdot f^*(x^*,y^*) \cdot dx \cdot dy}{\sqrt{\int_{\Delta M} f(x,y)^2 \cdot dx \cdot dy \cdot \int_{\Delta M} f^*(x^*,y^*)^2 \cdot dx \cdot dy}} \quad (4)$$

Where,  $\Delta M$  represent the surface of the pattern in the initial picture.

### 2.2.3. Research of the displacement field

The originality of this method is the following way of researching the displacement field. Consider a pattern centred in  $P$  and tops  $A$ ,  $B$ ,  $C$ ,  $D$  (figure 1). The correlation calculations will be done on the fours patterns centred in  $A$ ,  $B$ ,  $C$ , and  $D$  with the following assumption : their strain field are identical to the one of the pattern centred in  $P$ . These calculations are going to determine the rigid body displacement of the point  $A$ ,  $B$ ,  $C$ , and  $D$  which will be used to obtain all the terms of the strain field for the pattern centred in  $P$ . The exact solution from a numeric point of view will be determined with the help of an iterative process : the rigid body displacement of the points  $A$ ,  $B$ ,  $C$ , and  $D$  will be searched during the iteration 'i' with the help of the components of the strain field obtained at the iteration '(i-1)'. At the beginning of the iterative process, a rough initial solution for the two components of the displacement field is given

for the pattern. The strain field inside this pattern centred in P is therefore reduced, at the first iteration, to the rigid body displacement terms only, because the strain terms are considered initially equal to zero. The new position for the points A\*, B\*, C\*, and D\* in the final picture are searched successively for this first iteration with the help of the previous strain field. This research is done by scanning following x and y. The accurate position of the new coordinates of the points is obtained by the decreasing evolution simultaneously of the scan size area and the scan step. These displacements which allow to obtain a minimal correlation coefficient are noted  $du_{A1}$  and  $dv_{A1}$  for the point A and respectively,  $du_{B1}$ ,  $dv_{B1}$ ,  $du_{C1}$ ,  $dv_{C1}$ ,  $du_{D1}$ ,  $dv_{D1}$ , for the points B, C, D. With this eight values, the displacement field in P is obtained by a bilinear interpolation. The rigid body displacement calculation is continued until the following stability is reached :

$$|du_{Pn} - du_{P(n-1)}| \leq \varepsilon \quad \text{and} \quad |dv_{Pn} - dv_{P(n-1)}| \leq \varepsilon \quad \text{with} \quad \varepsilon = 0.01 \text{ pixel} \quad (5)$$

In the case where the iterative process would not converge, it is stopped at the 10 th iteration and the pattern is wrong and will not be taken into account for the strain calculation. Then, an interpolation allows to find the missing points after the displacement field calculations. The displacement field being obtained for this first pattern, the solution for the neighbours has to be searched in order to obtain the solution for the whole picture. Consequently, all the patterns surrounding this first pattern, will take its displacement field as initial solution.

#### 2.2.4. Research of the strain field

The strains calculation could be done for one pattern or for a group of patterns. This calculation will use the deformation gradient F and the Green-Lagrangian tensor E [7] :

$$[F] = \begin{bmatrix} F_{11} & F_{12} \\ F_{21} & F_{22} \end{bmatrix} \quad \text{and} \quad E = \frac{1}{2} \cdot ({}^T F \cdot F - I) \quad (6)$$

With this components, the main strain are given by :

$$\begin{cases} \varepsilon_I = \ln(E_{11} + E_{22} + \sqrt{(E_{11} - E_{22})^2 + (2 \cdot E_{12})^2} + 1) \\ \varepsilon_{II} = \ln(E_{11} + E_{22} - \sqrt{(E_{11} - E_{22})^2 + (2 \cdot E_{12})^2} + 1) \end{cases} \quad (7)$$

The angle between the first main strain axis and the picture axis x is given by :

$$\Phi = \text{Atn} \left[ \frac{2 \cdot E_{12} \cdot \sqrt{\ln(E_{11} + E_{22} + \sqrt{(E_{11} - E_{22})^2 + (2 \cdot E_{12})^2} + 1)}}{E_{11} - E_{22} + \sqrt{(E_{11} - E_{22})^2 + (2 \cdot E_{12})^2} + 1} \right] \quad (8)$$

### **2.3. Computer implementation**

From an initial and final picture, the user could define one or several studied areas. Only one operation is necessary to start the iterative process : give the first solution with the mouse. The algorithm is programmed in several languages : Fortran on workstation, C and Fortran on a PC (Windows 3.11, 95 and NT). Several results are available at the end of the calculations : the displacement field following x and y axis, the strain field following x and y axis, the deformed mesh and a vectorial representation of the displacement field.

### **3. Experimental apparatus**

This correlation method requires a special equipment and few precautions. The analyzed picture must have the most random aspect as possible : each pattern must be different from each other. Usually, this speckle aspect is obtained by pulverization of white and black painting. The pictures are obtained with a numeric camera Kodak Mega Plus (1024\*1024 pixels). This high definition camera with square contiguous pixels is linked to an acquisition card Matrox PIP1280 connected by a PC 486 DX50. Each picture represents around 1 Mega byte. The lens is a NIKON one (Micro-NIKKOR). A constant light has to be put during the tests. For information, the computation time with a Pentium 90 is about 0.2 seconds for a pattern of 9 pixels square. This time reduces to 0.04 seconds for the same processing executed on a workstation HP735.

### **4. Applications**

The following applications are very various. They concern also the mechanic field, the geotechnical field and biomechanical field... The small and also large strains are treated with the same software. The cover field varies from 7 x 7 mm<sup>2</sup> until several m<sup>2</sup>.

#### **4.1. Measure on a subway model**

Researches on the interaction ground / tunnel are done with a simulation model for the ground behaviour around a tunnel [8]. The ground is replaced by 150,000 small rollers of 4 mm diameter and 50 mm depth. They are put on a width of 1500 mm and on a height of 1000 mm. The tunnel diameter could vary in order to simulate the compressive and uncompressiv stages. This model allows the calculation and the visualization of the analogical ground behaviour around the tunnel during the simulation of the digging phases. Figure 2 shows the experimental device. The CCD camera covers the total field : 1000 x 1500 mm<sup>2</sup>. The distance between the camera and the model is 15 m. The different reflections of the rollers give directly the random aspect. Only, on the tunnel, initially uniform, some stains are done with indelible pencil in order to make easier the correlation on the whole picture. An initial picture is captured as reference. Then, several pictures are considered for different stages of the opening of the mandrel. After the correlation treatment between two pictures,

various results are obtained. The deformed mesh informs immediately on the digging effect of a tunnel. The digging is shown on the figure 3 which give the deformed mesh. In this special application, the advantages of the technical correlation are various. The accuracy on the measure is very good  $50\text{ }\mu\text{m}$  for a cover field of  $1000 \times 1500\text{ mm}^2$ . The number of measured point is very important : 11400 points.

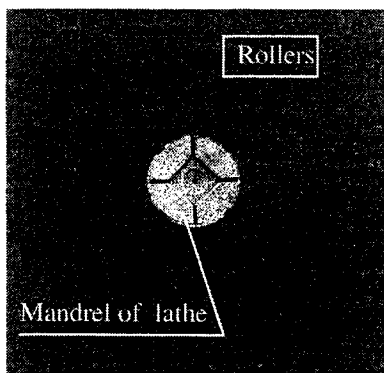


Figure 2 : Experimental device

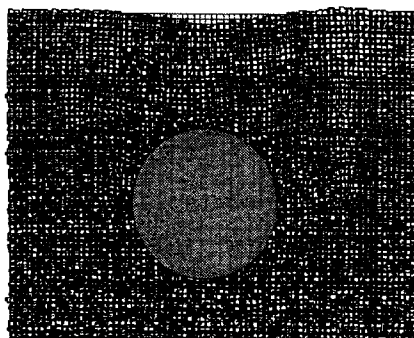


Figure 3 : Magnified deformed mesh

#### 4.2. Strain field for a XES steel in its plastic range under plane strain

A special specimen for a plane strain test is considered. The specimen width is 15.3 mm, its length is 31 mm and its thickness is 1 mm. The figure 4 shows the cover field by the CCD camera :  $160 \times 160\text{ mm}^2$ . An initial picture is taken as reference and another one for a specified load. After treatment by correlation, the following results are obtained. The deformed mesh is represented on figure 5.

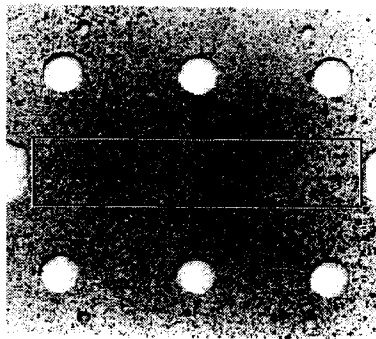


Figure 4 : Studied area on the specimen

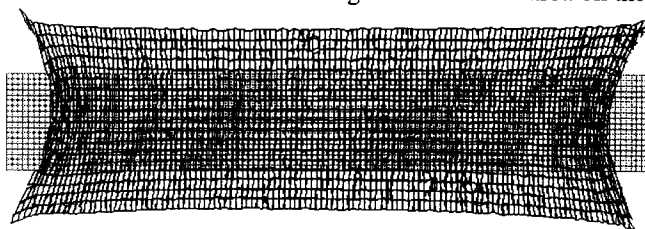


Figure 5 : Deformed mesh (Displacement x 20) and initial mesh

A strain rate of 5% following the vertical axis is calculated in the middle of the specimen. The transversal strain distribution is reproduced on the figure 6.

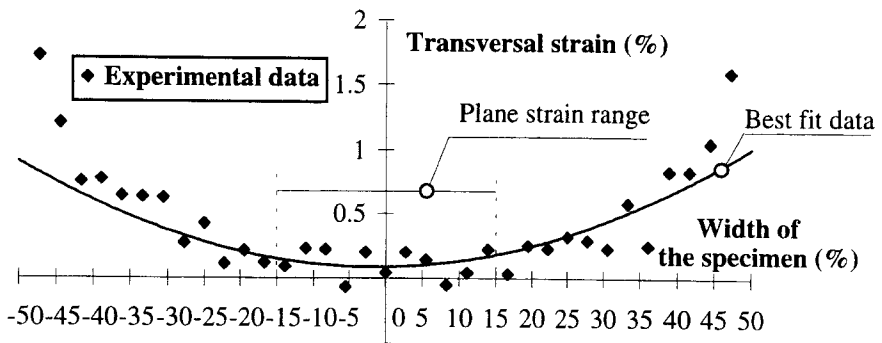


Figure 6 : Transversal strain distribution

This strain distribution underlines that the plane strain condition is only achieved on 30% of the total width. The advantages of this technical correlation for this special application are a good accuracy on the measure : 6  $\mu\text{m}$ , and a high density of measured points : 2124, giving a continuous information.

#### 4.3 Feasibility study on the strain field measurement for a bending specimen after an impact

Strains must be measured with the correlation method on a specimen tested in bending, after an impact. Two pictures are taken : before and after the impact. These pictures are then digitalized in order to be analyzed by correlation. The correlation calculations will be done only in the cranked section of the specimen. On the cranked section of the specimen the out-of-plane motion is small so that the measured in plane deformation are enough accurate. The strain field following the V axis is reported on the figure 7. A strain rate around 48% is measured by this method on the cranked section.

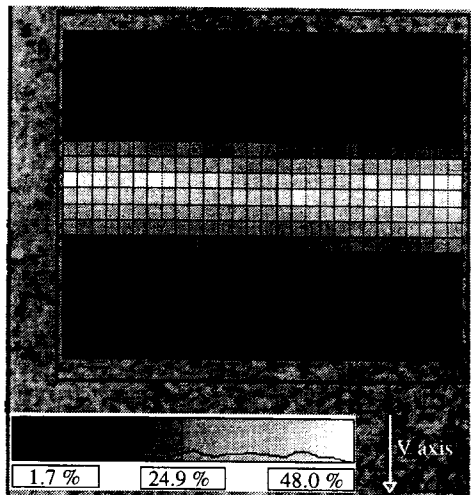


Figure 7 : Strain field following the v axis obtained by correlation

#### 4.4. Determination of Forming Limit Curves by correlation

The Marciniak test [9] is chosen for the experimental determination of Forming Limit Diagrams. Due to the special shape of the punch, the necking will occurs on the plane surface of the sheet so a technical correlation will be easily used. In order to simplify the experimental device (servo control of the camera in

order to maintain a stationary focal distance), a new apparatus was developed [10]. This drawing machine is designed for correlation technique. The experimental setup must also allow a sufficient lighting of the motif in order to obtain pictures of good quality. During the punch stroke, the sheet metal is stamped on the fixed punch. An inclined mirror at  $45^\circ$  restores the picture on the camera placed in front of the machine. The new structure allows to stamp sheets until a maximal depth of 45 mm. Due to the correlation technique, the classical markings (grids,...) are not used. A few seconds are required to make a simple deposit of white paint, followed by a pulverisation of black paint. An other advantage of this correlation technique is that the grid step could be changed at the beginning of the calculations. For the strain measurement on a sheet tested in metal forming, a pattern will be constituted by 8 or 12 pixels square. In this configuration, a pixel is around 0.07 mm, so the grid size could vary from 0.59 mm to 0.88 mm. Sheets are cut with different width in order to cover all the strain path. Then, the Marciniak's test is done until the necking occurs.

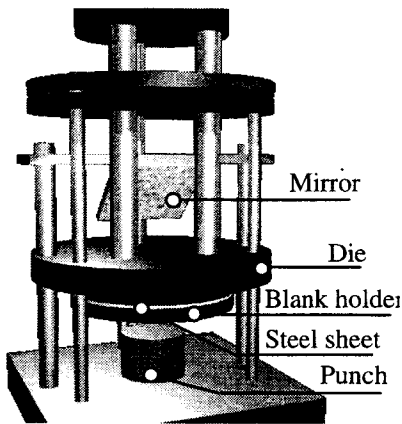


Figure 8 : New metal forming apparatus for the correlation technique

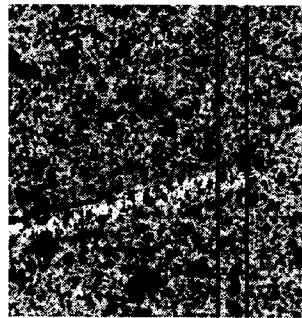


Figure 9 : Studied area near the necking

The case of the uniaxial traction is selected in order to illustrate the calculations. A area is taken perpendicularly to the necking line, figure 9. An initial picture is captured as reference. Then, the Marciniak test is started. At the necking occurrence, an other picture is taken. Then, the Braggard interpolation [9] is chosen for the measurement of the limit strain. The following F.L.D. is then obtained by correlation for an aluminium 5754 mild finish (See figure 10).



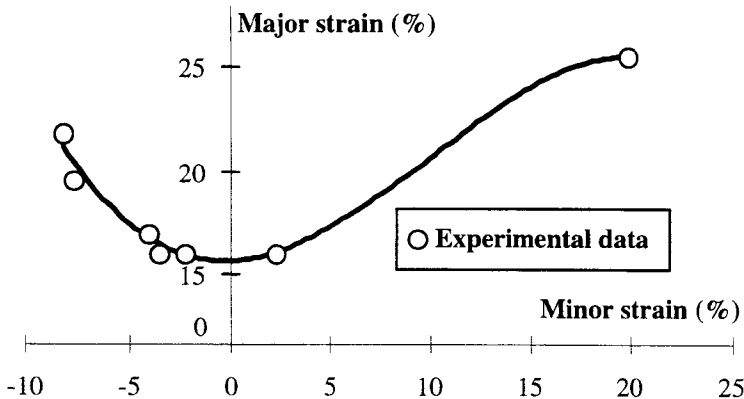


Figure 10 : F. L. D. obtained by correlation for aluminium 5754

Strain values around 25% are measured by this correlation technique. Thereafter, the forming limit curve for another materials are determined by correlation. A strain range of 80% is appreciated for a XES steel between two pictures. The advantages of this correlation technique for this application are various. First, classical marking are not needed which represents a big saving of time. Then, the computation time are strongly reduced due to the correlation algorithm. Also, the accuracy on the limit strain is improved.

#### 4.5. Mechanical characterization of human spongy bone.

A study concerning the osteoporosis for aged humans is realised. For this, it is necessary to measure mechanical characteristics. But, it is difficult to stick a strain gauge on the bone.

So, a correlation method is tried. Here, the speckle aspect is obtained by a graphite pulverization on the bone. The sample size is a bone cube of 7 mm per length. A compressive test is made. Then, several pictures are considered from different loads. After treatment, by the correlation software, the deformed mesh is obtained. The figure 11 underlines the bone fracture according two privileged directions. The accuracy on the result is about 0.5  $\mu\text{m}$ .

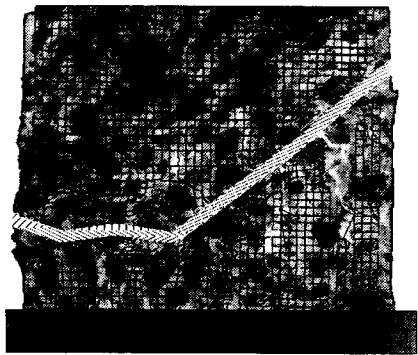


Figure 11 : Deformed mesh and enhanced fracture

#### 4.6. Tensile - compressive tests on rods

The unscrewing holding of carbon / steel rods tested in alternating tensile - compressive cycles is studied.

The relative unscrewing is appreciated with the correlation technique. The tests are achieved on a tensile machine (Schenck). The relative unscrewing between the steel sleeve and the carbon rod is measured, at the end of several cycles, with the correlation software. For each test, a reference picture is taken before the cycle, then this picture will be compared with a final picture. For this configuration, a pixel represents 0.46 mm. The accuracy is around 1/100 millimetre. The steel sleeve and the carbon rod are painted with black and white spray painting : figure 12. The rod is tested and each time, a relative unscrewing is found and measured. A unscrewing inferior to 1/10 millimetre can be estimated by this correlation technique.

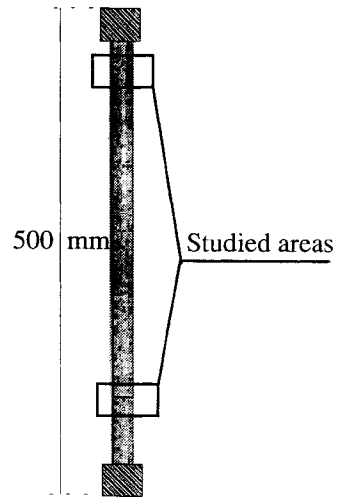


Figure 12 : Small rod

#### 4.7. Friction study on a punch during metal forming

A friction study on a punch during a metal forming [11] is managed. The Erichsen test is considered. The punch has a hemispherical form, the strain state is biaxial. The friction coefficient is directly bound to the strain distribution of the stamped sheet and to the strain on the pole of the stamped sheet. A pole is the first point in contact during the metal forming. A picture is considered as reference, then others during the metal forming.

The pole is well shown. The strain field gives a strain value of 5.2 % following the vertical axis and 4.7 % following the horizontal axis in the pole of the stamped sheet. The representation of the displacement field shows also the sheet pole. Because of the hemispherical form of the punch, the strain result, excepted for the pole, must be considered with care (it was shown before that an out of plane motion of 100 microns gives 232 micro strains).

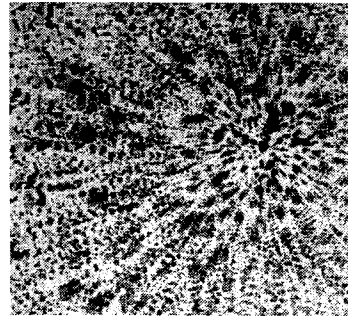


Figure 13 : Superimposition of two speckle pictures with different strain rate

#### 4.8. Determination of the Lankford coefficient

In order to take account the materials anisotropy, the Lankford's coefficient are used. They are obtained by a tensile test. If, x is the transversal direction then the Lankford's coefficient is :

$$r = \frac{d\epsilon_x}{d\epsilon_z} \quad (9)$$

So, with the incompressibility hypothesis :

$$r = -\frac{\epsilon_x}{\epsilon_x + \epsilon_y} \quad (10)$$

The Lankford coefficient for a XES steel is found by the correlation technique. A standardized specimen with a 20 mm width is previously painted. Then, an other picture after traction is considered, and, strains are calculated by correlation. For this special application of the determination of the Lankford coefficient, the computation time is very short because the correlation calculation will be done only on 4 small areas. The following result is found :  $r = 2.5$  which is well correlated with literature. The most advantage for this application is that effect border parasite is avoided during the measure which represents an improvement with regard to another manual method.

#### 4.9. Implantation study of prosthesis on calcaneum

The purpose of this application is to study the calcaneum, foot bone, and its fracture mechanisms [12]. To cure different fractures of calcaneum, a prosthesis by screwed plaques of the calcaneum fractures is proposed. Several pictures of the montage are considered for different values of compression load, and a first picture as reference. By correlation, the relative displacement of the fracture pieces is measured between different bones.



Figure 14: Displacements field

This technique gives valuable informations on the fragments displacement of the fracture and to make a choice between several prosthesis type.

#### 4.10. Study of a sensor for the biomechanical domain

In the biomechanical field, some characteristic, for example, the young modulus must be determined for human or animal bone. To this end, the following sensor is developed. Two gages are pasted on the wings of the sensor in order to convert strain information versus displacement measure, Figure 15:

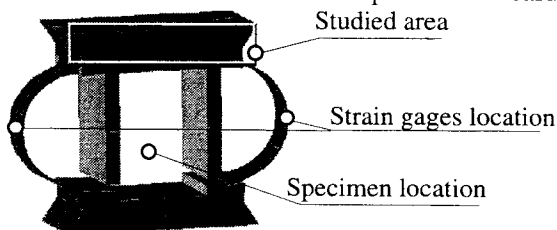


Figure 15 : Special sensor for bone characterization

In order to check this sensor, some tests are done, initially on aluminum and plexiglas specimens. Their young modulus are well known and the purpose is to recover these values with the sensor. But wrong results are found. The correlation technique is used here in order to see the sensor behaviour and also the specimen behaviour during the compressive test. For this reason, the specimen and also the sensor are covered with white and black painting. Then, a compressive test under small load is realised. Two pictures are considered and correlated.

The correlation calculations are done on the aluminum sample and on the sensor's top. The deformed mesh is represented on Figure 16 : the sample and the sensor are deformed. The correction of the sensor side are then achieved, which improves the next results. Finally, it is concluded that this sensor could work only with materials where the young modulus is small enough, for instance, when the young modulus ranges between 200 MPa (for the man) and 1500 MPa (for the sheep).

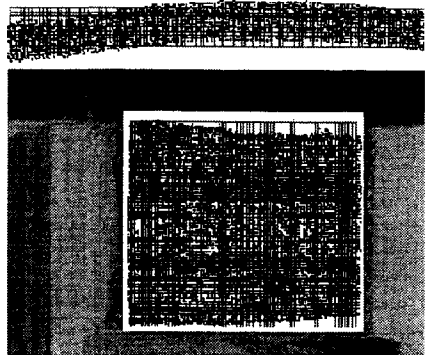


Figure 16 : Deformed mesh x 100 of the studied area and the specimen

#### **4.11. Determination of the rivers beds displacements**

The different impact conditions of drainage and solid apports, on the structure and the dynamic of substrate has to be studied experimentally and also, the invertebrates actions on the beds dynamic, and in particular by a sediment motion. A first study is achieved to decide if the correlation technique is enough efficient for this special application. So, the following test is managed. Some fine sand and stones are arranged on a stuff in a random manner. A picture is taken as reference. Then, the stuff is infinitesimally displaced in order to simulate for example a sediment river motion. The second picture being captured, the correlation algorithm is applied. The Figure 17 represents the displacement field following the vertical axis.

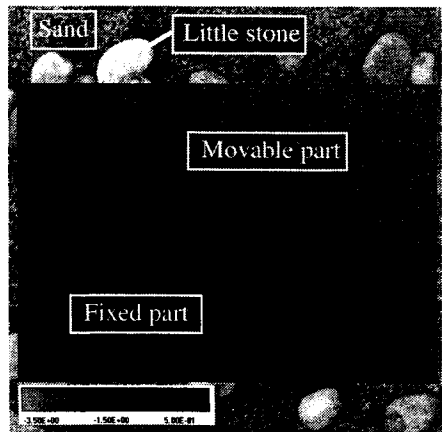


Figure 17 : Displacements field following the vertical axis

## 5. Discussion

Some points about the method utilization are underlined. First, the random aspect is not subjected to any modifications during the tests. A lost or a change of its aspect will carry on a wrong correlation. Afterwards, there is the lighting problem during the tests. A high contrast for the picture is required. So, a suitable lighting of the study area has to be set up. It has to ensure, principally, an uniform lighting of the studied area. A last point is still to be underlined. This particular point concerns directly the software utilization and principally the different correlation parameters adjustment. Indeed, there are five main correlation parameters : the correlation coefficient ( $C_1$  or  $C_2$ ), the grey level interpolation (bilinear or bi cubic spleen), pattern size (from 6 x 6 pixels to 35 x 35 pixels), grid size (from 6 x 6 pixels to 35 x 35 pixels), and, at last, the speckle aspect (fine or coarse). The parameter adjustment must be done in function of different situations : small or large strains, required accuracy, computation time... The developed software allows the user to make the choice between these different parameters, during the data entrance. For instance,  $C_2$  is used when the lighting changes between pictures. In the case of small strain, a large pattern and a bilinear interpolation give good results, although for large strain, small pattern and a bi cubic spleen interpolation are chosen to obtain best results. The grid size is adjust with the strain gradient : small grid size with large gradient, big grid size with small gradient...

## 6. Conclusion

The various tests described in this paper underlines the interest of this correlation technique for the displacement field measurement. This is a very powerful technique : strains until 80% are appreciated between two pictures. Nevertheless, improvements must be done. For example, the computation time must be reduced. More, it would be necessary to change the correlation algorithm in order to allow any area calculation : inclined rectangles, curved surfaces. An extension of this correlation technique for the 3D strain measurement is now in progress. Finally, this correlation technique has to become an another tool for measuring the displacement and / or strain field in special situations.

**Acknowledgements :** The authors thanks the Geotechnical Laboratory (Insa-Lyon), the car manufacturer Renault, C.E.A. (Commissariat à l'Energie Atomique), Biomechanical Laboratory (Insa-Lyon), Gec Alsthom company, Hôpital Sud de Grenoble, Région Rhône-Alpes and the Cemagref.

## 7. References

- [1] **Sutton, M. A., Wolters, W. J., Peters, W. H., Ranson, W. F., McNeill, S. R.** Determination of displacements using an improved digital correlation method, *Image and Vision Computing*, vol 1 n°3, août 1983, 133-139
- [2] **Pratt, W. K.** *Digital Image Processing*, Second Edition, Wiley-Interscience Publication, ISBN 0-471-85766-1, 112-117
- [3] **Sutton, M. A., Mingqi cheng, Peters, W. H., Chao, Y. S., McNeill S. R.** Application of an optimized digital correlation method to planar deformation analysis, *Image and Vision Computing*, vol 4 n°3, août 1986, 143-150
- [4] **Bruck, H. A., McNeill, S. R., Sutton, M. A., Peters, W. H.** Digital Image correlation using Newton-Raphson Method of Partial Differential correction, *Experimental Mechanics*, septembre 1989, 261-267
- [5] **Mguil - Touchal, S., Morestin, F., Brunet, M.** Mesure de champs de déformations par une méthode optique de corrélation directe d'images digitales, Actes du Colloque National Mécatmat, Mécanismes et Mécanique des grandes déformations, Aussois, 29 janvier-1er février 1996, 179-182
- [6] **Chu, T. C., Ranson, W. F., Sutton, M. A., Peters, W. H.** Application of Correlation Technique to Experimental Mechanics, *Experimental Mechanics*, septembre 1985, 232-244
- [7], Computerized Measurement Products Services, Spring/Summer 1994, 1223 People Avenue, TROY, NY 12180-3590
- [8] **Gachet, P., Galle, J. M.** Mesure des déplacements de sol analogique à l'aide du logiciel SIFASOFT (corrélation directe d'images digitales), P.F.E 1996, INSA de Lyon, Laboratoire U.R.G.C-Géotechnique
- [9] **Arrieux, R.** "Détermination théorique et expérimentale des Courbes Limites de Formage en contraintes", thèse d'état, INSA et UCLB1, 1990
- [10] **Schultze, Y.** Mesure par imagerie appliquée à la détermination des Coubes Limites de Formage des tôles, D.E.A 1995, INSA de Lyon, Laboratoire de Mécanique des Solides
- [11] **Burlat, M.** "Etude de faisabilité d'outil d'emboutissage par combinaison de différents matériaux", thèse en cours, INSA de Lyon
- [12] **Fournes, C.** Caractérisation mécanique d'ostéosynthèses des fractures du calcanéum et étude des propriétés de l'hydroxyapatite, P.F.E 1996, INSA de Lyon, Laboratoire de Mécanique des Solides